Journal of the European Ceramic Society 36 (2016) 247–251

Contents lists available at www.sciencedirect.com

Journal of the European Ceramic Society

journal homepage: www.elsevier.com/locate/jeurceramsoc

Short communication

A novel low-temperature fired microwave dielectric ceramic $BaMg_2V_2O_8$ with ultra-low loss

Yang Wang, Ruzhong Zuo*

Institute of Electro Ceramics & Devices, School of Materials Science and Engineering, Hefei University of Technology, Hefei 230009, PR China

ARTICLE INFO

Article history:
Received 3 August 2015
Received in revised form
11 September 2015
Accepted 12 September 2015
Available online 26 September 2015

Keywords:
Vanadate
Rietveld refinement
Microwave dielectric properties
Low-temperature sintering

ABSTRACT

A new ultra-low-loss microwave dielectric ceramic $BaMg_2V_2O_8$ with a tetragonal structure was successfully fabricated via a conventional solid-state method. X-ray diffraction and field-emission scanning electron microscopy were performed to explore the phase crystal, grain morphology and densification behavior. The results indicated that pure and dense $BaMg_2V_2O_8$ ceramics with dielectric constant $\epsilon_r = 12$, quality factor $Q \times f = 156140$ GHz (9.9 GHz) and the temperature coefficient of resonant frequency $\tau_f = -36$ ppm/°C could be yielded at a relatively low sintering temperature of 900 °C. Moreover, the $0.87BaMg_2V_2O_8$–$0.13TiO_2$ ceramic sintered at 900 °C for 4 h demonstrated a near-zero τ_f of −4 ppm/°C, an ϵ_r of 13 and a $Q \times f$ of 97,334 GHz (9.6 GHz), showing large application potentials.

1. Introduction

The past decades have witnessed revolutionary changes in mobile phone system, which continuously increased the demand for novel high-performance microwave devices [1]. Accordingly, dielectric materials with a low dielectric constant (ϵ_r), a high quality factor ($Q \times f$) and a near-zero temperature coefficient of resonant frequency (τ_f) have attracted lots of attention in microwave circuits, substrates and passive components [2,3]. Particularly, low-temperature cofired ceramic (LTCC) technology has been widely applied for the fabrication of miniaturized and integrated microwave devices, which made it extremely significant to develop potential candidates with sintering temperatures lower than the melting point of Ag (961 °C). Up to date, a mass of low-ϵ_r microwave ceramic materials with desirable properties have been developed, however, most of them were ruled out of practical applications in LTCC-based devices owing to their high densification temperatures and undesirable τ_f values [4–8]. Recently, some Li_2O-, TeO_2-, Bi_2O_3-, and MoO_3-based compounds with intrinsically lower sintering temperatures have been extensively studied in this context [9–13]. Vanadate compounds with excellent microwave dielectric properties have been also developed as low-firing ceramics and some of them proved to be chemically compatible with Ag electrode [14–17].

$BaMg_2V_2O_8$ was referred to as an impurity phase as a result of chemical reactions between two phases in the $Mg_3(VO_4)_2$–$xBa_3(VO_4)_2$ ($x = 0$–1) composite ceramics [18], in which unusually enhanced $Q \times f$ value at $x = 0.2$ seemed to be unclearly understood. It was encouraged to anticipate excellent microwave dielectric properties of pure-phase $BaMg_2V_2O_8$ compound. Being isotypic with $BaCo_2V_2O_8$, $BaMg_2V_2O_8$ belongs to a wide group of so-called quasi-one-dimensional (Q1D) antiferromagnets [19]. All magnetic Mg^{2+} ions are equivalent with arrays of edge-sharing MgO_6 octahedra forming screw-chains along c-axis, as schematically shown in Fig. 1 [20]. The screw-chains are separated by nonmagnetic VO_4 (V^{5+}) tetrahedra and the Ba^{2+} ions. The purpose of present work was to fabricate pure-phase $BaMg_2V_2O_8$ ceramics via a conventional solid-state ceramic route. The phase crystal, sintering behavior, microstructure and especially microwave dielectric properties were investigated in detail for the first time.

2. Experimental

The $BaMg_2V_2O_8$ ceramic was synthesized by a conventional solid-state reaction route using high-purity powders of $Ba(OH)_2{\cdot}8H_2O$, MgO and V_2O_5. Stoichiometric amounts of chemical powders were weighed and ball-milled for 4 h using zirconia balls in alcohol medium. The resulting slurry was then rapidly dried and calcined at 800 °C for 4 h to obtain $BaMg_2V_2O_8$ powders. The calcined powders were re-milled for 6 h and then mixed together with 5 wt% PVA as a binder. The granulated powders were subsequently pressed into cylinders with dimensions of 10 mm in

* Corresponding author. Fax: +86 551 62905285.
E-mail addresses: rzzuo@hotmail.com, piezolab@hfut.edu.cn (R. Zuo).

http://dx.doi.org/10.1016/j.jeurceramsoc.2015.09.011
0955-2219/

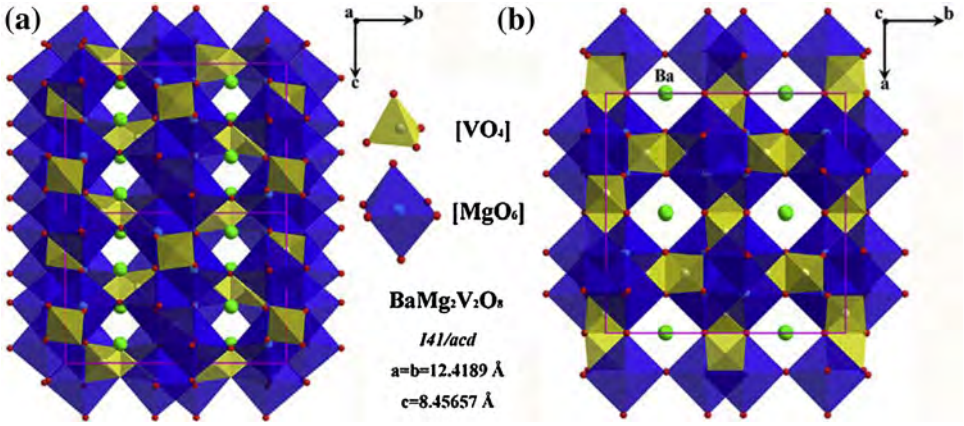

Fig. 1. The crystal structure of $BaMg_2V_2O_8$ seen along (a) a-axis and (b) c-axis (reproduced by permission from John Wiley & Sons).

diameter and 7–8 mm in height. The specimens were first heated at 550 °C in air for 4 h to remove the organic binder and then sintered at 870–930 °C for 4 h. To tailor its negative τ_f, 9–15 vol% TiO_2 were mixed with as-prepared pure-phase $BaMg_2V_2O_8$ powders, and then sintered at 870–945 °C for 4 h.

The crystal structure of the fired ceramics was identified via an X-ray diffractometer (XRD, D/Max2500 V, Rigaku, Japan) using Cu*K*α radiation. The structural parameters were obtained from Rietveld refinement of the XRD data using the GSAS-EXPGUI program. The refinement involved the lattice parameters, background, atomic coordinates, site occupancies and isotropic thermal parameters as well as profile parameters (peak height and peak shape) [21]. High-resolution X-ray photoelectron spectroscopy (XPS, ESCALAB250, Thermo, USA) was utilized to determine the valence states of vanadium ions. The bulk densities of the sintered ceramics were measured by the Archimedes method. The polished and thermally etched surfaces of the pellets were observed using a field-emission scanning electron microscope (FE-SEM; SU8020, JEOL, Tokyo, Japan). The evaporation loss of V_2O_5 was evaluated by measuring the mass change of the samples before and after sintering. Microwave dielectric properties of sintered ceramics were measured using a network analyzer (N5230C, Agilent, Palo Alto, CA) and a temperature chamber (GDW-100, Saiweisi, Changzhou, China). The τ_f values of the samples were measured in the temperature range from 20 °C to 80 °C and calculated by the following equation:

$$\tau_f = \frac{f_2 - f_1}{f_1 (T_2 - T_1)} \quad (1)$$

where f_1 and f_2 represent the resonant frequencies at T_1 and T_2, respectively.

3. Results and discussion

Fig. 2 depicts XRD patterns of $BaMg_2V_2O_8$ ceramics sintered at different temperatures for 4 h. Evidently, the diffraction peaks of $BaMg_2V_2O_8$ could be well indexed based on JCPDS file number 72-2159 with a tetragonal structure (space group I41/*acd*) and no trace of secondary phases were detected, indicating the formation of pure-phase $BaMg_2V_2O_8$. The lattice parameters and reliability factors of all studied samples after the Rietveld refinement are listed in Table 1. It can be seen that there was no any obvious systematic variation in lattice parameters and cell volumes with increasing firing temperatures. Their values kept good consistency with those previously reported [20].

Fig. 3 shows SEM images of polished and thermally etched $BaMg_2V_2O_8$ ceramics sintered at different temperatures: It is evident that $BaMg_2V_2O_8$ ceramics could be well densified within a certain temperature range of 885–915 °C and exhibited a fine grain morphology (~3 μm in average grain size). However, the sample density seemed to decrease as it was sintered at 930 °C, probably owing to the V_2O_5 evaporation. Table 2 gives the weight-loss analysis of $BaMg_2V_2O_8$ ceramics after sintering at different temperatures, which can be generally ascribed to the evaporation of V_2O_5 in this system [17,22]. Obviously, its evaporation loss became more serious at higher sintering temperatures.

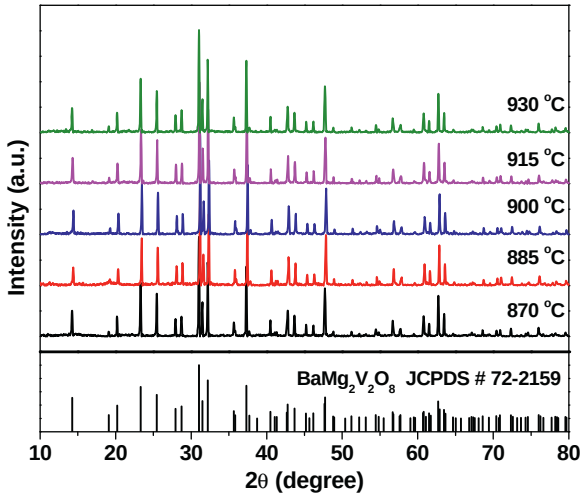

Fig. 2. XRD patterns of $BaMg_2V_2O_8$ ceramics sintered at 870–930 °C for 4 h.

Fig. 4 illustrates the variation of relative density, packing fraction (f) and microwave dielectric properties of $BaMg_2V_2O_8$ ceramics as a function of sintering temperature. Obviously, all samples exhibited high relative densities (>95%), keeping consistent with the microstructural observation. With increasing firing temperatures, the relative density firstly increased and reached the optimum value at 915 °C, then decreased slightly, which kept good consistency with the microstructural observation. Moreover, ϵ_r was found to keep the same variation trend with temperature as the relative density, indicating that porosity acts as a main controlling factor of dielectric constant. By comparison, Q × f values continuously increased to a maximum value of 156,140 GHz at 900 °C, and then decreased with further increasing firing temperatures. The decrease of Q × f values at higher firing temperatures might be due to the volatilization of V_2O_5 as mentioned above. Moreover, the change of valence states of V^{5+} ions might make an additional contribution. The XPS analysis of $BaMg_2V_2O_8$ ceramics after sintering was carried out, as shown in Fig. 5. The XPS spectra of V 2p

Table 1
Refined unit cell volume, reliability factors, goodness-of-fit indicator of $BaMg_2V_2O_8$ ceramics at different sintering temperatures.

S.T. (°C)	Lattice parameters (Å)		Unit cell volume (Å^3)	R_{wp} (%)	R_p (%)	X^2
	a = b	c				
870	12.4165(2)	8.4604(7)	1304.3(3)	9.28	6.76	1.557
885	12.4136(1)	8.4590(4)	1303.5(3)	8.67	5.94	1.681
900	12.4130(2)	8.4579(6)	1303.2(2)	8.75	6.59	1.435
915	12.4160(1)	8.4596(5)	1304.1(2)	8.42	6.19	1.588
930	12.4169(2)	8.4609(5)	1304.5(3)	8.95	6.52	1.612

S.T.: sintering temperature; R_{wp}: the reliability factor of weighted patterns; R_p: the reliability factor of patterns; χ^2 goodness-of-fit indicator = $(R_{wp}/R_{exp})^2$.

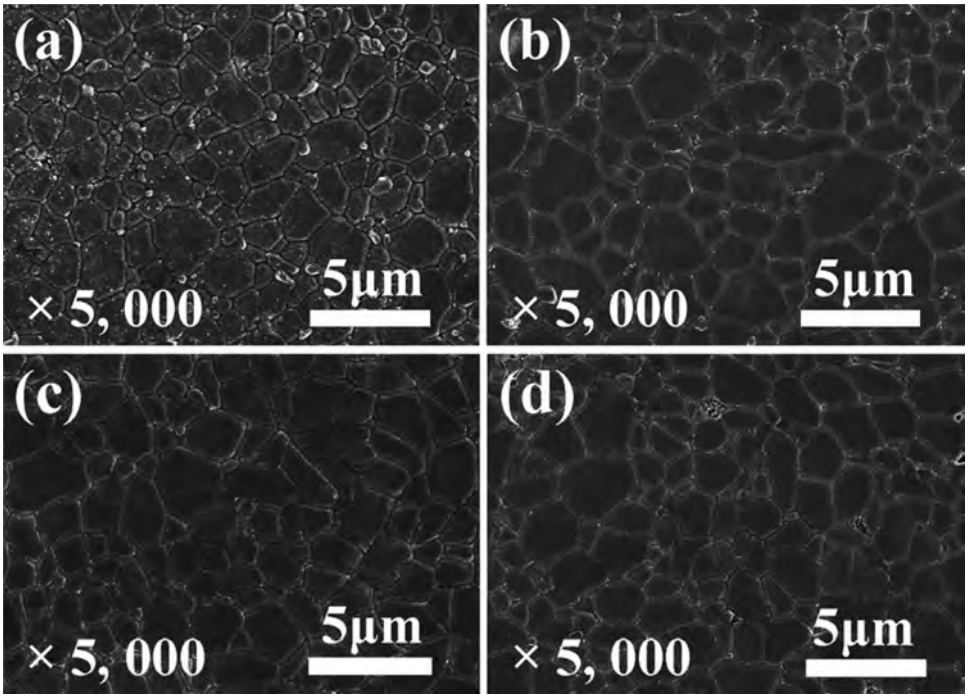

Fig. 3. SEM images of polished and thermally etched $BaMg_2V_2O_8$ ceramics sintered at different temperatures: (a) 885 °C, (b) 900 °C, (c) 915 °C, and (d) 930 °C for 4 h.

Table 2
Weight loss and content of vanadium ions with different valence states in $BaMg_2V_2O_8$ ceramics after sintering at different sintering temperatures.

S.T. (°C)	Weight loss (%)	Vanadium ion content (mol%)	
		V^{5+}	V^{4+}
870	0.15 ± 0.04	98.7	1.3
900	0.27 ± 0.03	96.4	3.6
930	0.36 ± 0.03	91.2	8.8

region were further handled by subtracting the background with the Shirley method. By using the Gaussian–Lorentzian curve fitting, the V $2p_{3/2}$ peak was found to be split into two peaks of V^{5+} and V^{4+}, whose positions agreed well with reported values [23]. Of note is that the V^{4+} content was quite low and almost neglectable for samples sintered at 870 °C and 900 °C. However, as firing temperatures increased up to 930 °C, V^{4+} content increased apparently, as shown in Table 2. Similar results were also demonstrated in our previous work and also in $Ca_5Co_4(VO_4)_6$ ceramics [17,22], indicating that vanadate compounds are prone to volatilize easily and possess variable valences at higher temperatures, which might exert negative influences on the Q × f values.

Generally, both intrinsic loss from lattice vibration modes and extrinsic loss from secondary phases, oxygen vacancies, grain sizes and porosity contribute to the experimentally measured microwave dielectric loss [24]. Considering that pure-phase $BaMg_2V_2O_8$ exhibited a uniform morphology and a relatively high relative density, their impacts on Q × f could thus be neglected. The evaporation loss of V_2O_5 or the change of ionic valence states must bring about the stoichiometric deviation and atomic vacancies, thus inducing additional dielectric loss. A parameter, packing fraction (f) was believed to be closely correlated with the Q × f value [25], which was defined using a division of the sum of the packed ions (V_{PI}) volume over a primitive unit cell (V_{PUC}) volume, as expressed by the following equation:

$$f(\%) = \frac{V_{PI}}{V_{PUC}} \times Z \quad (2)$$

where Z is the number of atoms per unit cell. The results in Fig. 5 indicated a strong dependence of the Q × f on the packing fraction because the increase in packing fraction can weaken lattice vibrations. Moreover, it can be seen that sintering temperature exerted

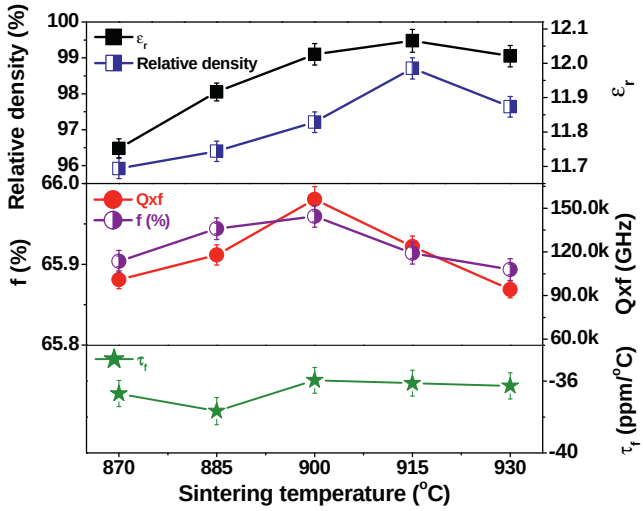

Fig. 4. The variation of relative density, packing fraction and microwave dielectric properties of $BaMg_2V_2O_8$ ceramics as a function of sintering temperature.

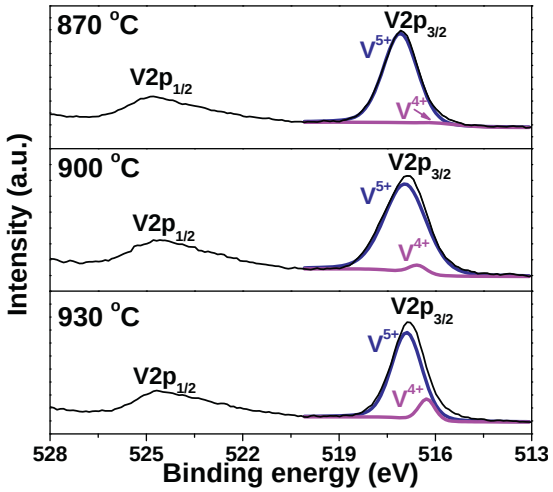

Fig. 5. XPS spectra of V 2p region in $BaMg_2V_2O_8$ ceramics sintered at 870 °C, 900 °C, and 930 °C for 4 h.

no apparent influence on the τ_f value and it remained in a narrow range from −36 ppm/°C to −37.7 ppm/°C since there was no composition or structure change with changing firing temperature.

Compared with other low-temperature fired and low-ϵ_r microwave dielectric materials, such as $Li_2Zn_2Mo_3O_{12}$ ($\epsilon_r = 11.1$, $Q \times f = 70{,}000$ GHz and $\tau_f = -90$ ppm/°C) [26], $LiCa_3MgV_3O_{12}$ ($\epsilon_r = 10.5$, $Q \times f = 74{,}700$ GHz and $\tau_f = -61$ ppm/°C) [27], $Ca_2Zn_4(VO_4)_6$ ($\epsilon_r = 11.7$, $Q \times f = 49{,}400$ GHz and $\tau_f = -83$ ppm/°C) [28] and $Ba_3V_4O_{13}$ ($\epsilon_r = 9.6$, $Q \times f = 56{,}100$ GHz and $\tau_f = -42$ ppm/°C) [29], the $BaMg_2V_2O_8$ ceramic in present study demonstrated a much higher $Q \times f$ value and a moderate τ_f value. However, considering that a negative τ_f value that $BaMg_2V_2O_8$ owns was not desirable for practical applications, rutile TiO_2 with a large positive τ_f value was employed as a τ_f-modifier. The microwave dielectric properties of $(1-x)BaMg_2V_2O_8$–$xTiO_2$ ($0 \le x \le 0.15$) ceramics sintered at their optimum temperatures are listed in Table 3. Although $Q \times f$ was slightly sacrificed, a near-zero τ_f could be achieved. The 13% TiO_2 added $BaMg_2V_2O_8$ ceramics fired at 900 °C for 4 h exhibited excellent microwave dielectric properties of $\epsilon_r = 13$, $Q \times f = 97334$ GHz (9.6 GHz) and $\tau_f = -4$ ppm/°C, demonstrating large application potentials.

Table 3
Microwave dielectric properties of $(1-x)$ $BaMg_2V_2O_8$–xTiO2 ceramics.

x	S.T. (°C)	ϵ_r	$Q \times f$ (GHz)	τ_f (ppm/°C)
0	900	12 ± 0.03	156140 ± 8807	−36 ± 0.7
0.09	870	12.7 ± 0.03	117322 ± 5488	−22.3 ± 0.5
0.11	885	12.8 ± 0.04	101174 ± 4841	−14.5 ± 0.3
0.13	900	13 ± 0.04	97334 ± 4808	−4.6 ± 0.1
0.15	915	13.2 ± 0.04	76601 ± 4357	11.6 ± 0.3

4. Conclusions

In this study, a novel low-temperature fired microwave dielectric ceramic $BaMg_2V_2O_8$ with a tetragonal structure was successfully prepared by a standard solid-state reaction method. The pure-phase compound with a homogeneous and dense microstructure exhibited an ϵ_r of 12, an ultra-high $Q \times f$ of 156,140 GHz (9.9 GHz), and a τ_f of −36 ppm/°C as sintered at 900 °C for 4 h. Rutile TiO_2 was introduced to tailor its negative τ_f value. The $0.87BaMg_2V_2O_8$–$0.13TiO_2$ sample sintered at 900 °C for 4 h demonstrated excellent dielectric properties of $\epsilon_r = 13$, $Q \times f = 97{,}334$ GHz (9.6 GHz) and $\tau_f = -4$ ppm/°C.

Acknowledgements

Financial support from the National Natural Science Foundation of China (Grant No. 51272060) and the Anhui Provincial Natural Science Foundation (1508085JGD04) is gratefully acknowledged.

References

[1] T.A. Vanderah, Talking ceramics, Science 298 (2002) 1182–1184.
[2] H.T. Wu, Y.S. Jiang, Y.L. Yue, Low-temperature synthesis and microwave dielectric properties of trirutile-structure $MgTa_2O_6$ ceramics by aqueous sol–gel process, Ceram. Int. 38 (2012) 5151–5156.
[3] C. Jiang, S.P. Wu, W.P. Tu, L. Jiao, Z.O. Zeng, Synthesis of (Zn, Mg)TiO_3–TiO_2 composite ceramics for multilayer ceramic capacitors, Mater. Chem. Phys. 124 (2010) 347–352.
[4] N.M. Alford, S.J. Penn, Sintered alumina with low dielectric loss, J. Appl. Phys. 80 (1996) 5895–5898.
[5] J.C. Kim, M.H. Kim, J.B. Lim, S. Nahm, J.H. Paik, J.H. Kim, Synthesis and microwave dielectric properties of $Re_3Ga_5O_{12}$ (Re: Nd, Sm,Eu, Dy, Yb, and Y) ceramics, J. Am. Ceram. Soc. 90 (2007) 641–644.
[6] C.W. Zheng, S.Y. Wu, X.M. Chen, K.X. Song, Modification of $MgAl_2O_4$ microwave dielectric ceramics by Zn substitution, J. Am. Ceram. Soc. 90 (2007) 1483–1486.
[7] K.P. Surendran, N. Santha, P. Mohanan, M.T. Sebastian, Temperature stable low loss ceramic dielectrics in $(1-x)ZnAl_2O_4$–$xTiO_2$ system for microwave substrate applications, Eur. Phys. J. B 41 (2004) 301–306.

[8] D. Zhou, C.A. Randall, L.X. Pang, H. Wang, J. Guo, G.Q. Zhang, X.G. Wu, L. Shui, X. Yao, Microwave dielectric properties of Li_2WO_4 ceramic with ultra-low sintering temperature, J. Am. Ceram. Soc. 94 (2011) 348–350.
[9] G. Subodh, R. Ratheesh, M.V. Jacob, M.T. Sebastian, Microwave dielectric properties and vibrational spectroscopic analysis of $MgTe_2O_5$ ceramics, J. Mater. Res. 23 (2008) 1551–1556.
[10] D. Zhou, H. Wang, L.X. Pang, C.A. Randall, X. Yao, Bi_2O_3–MoO_3 binary system: an alternative ultralow sintering temperature microwave dielectric, J. Am. Ceram. Soc. 92 (2009) 2242–2246.
[11] D. Zhou, L.X. Pang, J. Guo, G.Q. Zhang, Y. Wu, H. Wang, X. Yao, Low temperature firing microwave dielectric ceramics $(K_{0.5}Ln_{0.5})MoO_4$ (Ln = Nd and Sm) with low dielectric loss, J. Eur. Ceram. Soc. 31 (2011) 2749–2752.
[12] A. Surjith, R. Ratheesh, High Q ceramics in the $ACe_2(MoO_4)_4$ (A = Ba, Sr and Ca) system for LTCC applications, J. Alloys Compd. 550 (2013) 169–172.
[13] M.R. Joung, J.S. Kim, M.E. Song, S. Nahm, J.H. Paik, Formation process and microwave dielectric properties of the $R_2V_2O_7$ (R = Ba, Sr and Ca) ceramics, J. Am. Ceram. Soc. 92 (2009) 3092–3094.
[14] L. Fang, C.X. Su, H.F. Zhou, Z.H. Wei, H. Zhang, Novel low-firing microwave dielectric ceramic $LiCa_3MgV_3O_{12}$ with low dielectric loss, J. Am. Ceram. Soc. 96 (2013) 688–690.
[15] R. Umemura, H. Ogawa, H. Ohsato, A. Kan, A. Yokoi, Microwave dielectric properties of low-temperature sintered $Mg_3(VO_4)_2$ ceramic, J. Eur. Ceram. Soc. 25 (2005) 2865–2870.
[16] L. Fang, H.H. Guo, W.S. Fang, Z.H. Wei, C.C. Li, BaTa2V2O11: a novel low fired microwave dielectric ceramic, J. Eur. Ceram. Soc. 35 (2015) 3765–3770.
[17] Y. Wang, R.Z. Zuo, C. Zhang, J. Zhang, T.W. Zhang, Low-temperature-fired $ReVO_4$ (Re = La, Ce) microwave dielectric ceramics, J. Am. Ceram. Soc. 98 (2015) 1–4.
[18] H. Ogawa, A. Yokoi, R. Umemura, A. Kan, Microwave dielectric properties of $Mg_3(VO_4)_2$–$Ba_3(VO_4)_2$ ceramics for LTCC with near zero temperature coefficient of resonant frequency, J. Eur. Ceram. Soc. 27 (2007) 3099–3104.
[19] Z.Z. He, D.S. Fu, T. Kŷomen, T. Taniyama, M. Itoh, Crystal growth and magnetic properties of $BaCo_2V_2O_8$, Chem. Mater. 17 (2005) 2924–2926.
[20] R. Wichmann, H. Müller-Buschbaum, Neue verbindungen mit $SrNi_2V_2O8$-struktur: $BaCo_2V_2O_8$ und $BaMg_2V_2O_8$, Z. Anorg. Allg. Chem. 534 (1986) 153–158.
[21] A.C. Larson, R.B. Von Dreele, General Structure Analysis System, Los Alamos National Laboratory Report No. LAUR, 2004, p. 86.
[22] G.G. Yao, P. Liu, X.G. Zhao, J.P. Zhou, H.W. Zhang, Low-temperature sintering and microwave dielectric properties of $Ca_5Co_4(VO_4)_6$ ceramics, J. Eur. Ceram. Soc. 34 (2014) 2983–2987.
[23] M.C. Biesinger, L.W.M. Lau, A.R. Gerson, R.S.C. Smart, Resolving surface chemical states in XPS analysis of first row transition metals, oxides and hydroxides: Sc, Ti, V, Cu and Zn, Appl. Surf. Sci. 257 (2010) 887–898.
[24] Y.C. Chen, Y.N. Wang, C.H. Hsu, Enhancement microwave dielectric properties of Mg_2SnO_4 ceramics by substituting Mg^{2+} with Ni^{2+}, Mater. Chem. Phys. 133 (2012) 829–833.
[25] E.S. Kim, B.S. Chun, R. Freer, R.J. Cernik, Effects of packing fraction and bond valance on microwave dielectric properties of $A^{2+}B^{6+}O_4$ (A^{2+}: Ca, Pb, Ba; B^{6+}: Mo, W) ceramics, J. Eur. Ceram. Soc. 30 (2010) 1731–1736.
[26] D. Zhou, C.A. Randall, L.X. Pang, H. Wang, X.G. Wu, J. Guo, G.Q. Zhang, L. Shui, X. Yao, Microwave dielectric properties of $Li_2(M^{2+})_2Mo_3O_{12}$ and $Li_3(M^{3+})Mo_3O_{12}$ (M = Zn, Ca, Al, and In) lyonsite-related-type ceramics with ultra-low sintering temperatures, J. Am. Ceram. Soc. 94 (2011) 802–805.
[27] L. Fang, C.X. Su, H.F. Zhou, Z.H. Wei, H. Zhang, Novel low-firing microwave dielectric ceramic $LiCa_3MgV_3O_{12}$ with low dielectric loss, J. Am. Ceram. Soc. 96 (2013) 688–690.
[28] G.G. Yao, P. Liu, H.W. Zhang, Novel series of low-firing microwave dielectric ceramics: $Ca_5A_4(VO_4)_6$ (A^{2+} = Mg, Zn), J. Am. Ceram. Soc. 96 (2013) 1691–1693.
[29] S.E. Kalathil, U.A. Neelakantan, R. Ratheesh, Microwave dielectric properties of ultralow-temperature cofirable $Ba_3V_4O_{13}$ ceramics, J. Am. Ceram. Soc. 97 (2014) 1530–1533.